Electric Power Systems Research 116 (2014) 408–418

Contents lists available at ScienceDirect

Electric Power Systems Research

journal homepage: www.elsevier.com/locate/epsr

A risk-averse security-constrained optimal power flow for a power grid subject to hurricanes

Pirooz Javanbakht*, Salman Mohagheghi

Department of Electrical Engineering and Computer Science, Colorado School of Mines, 1610 Illinois Street, Golden, CO 80401, USA

ARTICLE INFO

Article history:
Received 3 May 2014
Received in revised form 17 June 2014
Accepted 10 July 2014
Available online 1 August 2014

Keywords:
Contingency analysis
Generation dispatch
Hurricanes
Natural disasters
Optimal power flow
Risk analysis

ABSTRACT

During the course of a hurricane, many components in the power grid may be affected. In particular, loss of transmission lines and/or towers due to excess wind conditions may adversely impact the operation of the grid and force a re-dispatch of the generation units. However, large generation units have considerable ramp rates and usually are not able to vary their outputs fast enough. This might lead to temporary imbalances between load and generation that, if not resolved quickly, may result in more severe cascading failures. When a large scale disturbance such as a hurricane is forthcoming it is most beneficial to proactively dispatch the grid so as to minimize the likelihood of future failures. To assist the operator in proactively responding to an imminent event such as a hurricane, a risk-averse generation dispatch model is presented in this paper based on security-constrained AC optimal power flow. To perform (N–k) contingency analysis, a geospatial model of the power grid is developed that allows for the computation of outage probabilities of the transmission lines affected by the hurricane wind fields. Statistical analysis has been performed on the historical data on the past hurricane events in the US in order to simulate realistic hurricane scenarios. The IEEE 118-bus test system has been mapped onto the map of the state of Texas in order to provide a realistic test bed. The proposed algorithm takes into account the cost of operation, as well as the risks associated with overload and over/undervoltage conditions. Moreover, it allows for preventive as well as corrective dispatch of the power grid.

1. Introduction

Natural disasters have been considered as one of the two main causes of the largest blackouts in North America (the other being cascading failures) [1]. As one of the most severe types of natural disaster events, a hurricane can cause major damage and devastation to the critical infrastructure of the affected cities. When it comes to hurricanes, power grids are not necessarily immune and have been shown to be severely affected in the past [1–3]. High winds can potentially damage the overhead lines and towers/poles, while high floodwater as a result of heavy rains and hurricane surge may lead to flooding of substations. The colossal amount of destructive energy released during the course of a high-intensity hurricane makes it impractical, if not infeasible, to guarantee the continuous secure operation of all grid components. At the same time, the uncertain and infrequent nature of the event prevents utilities from reinforcing the grid through conservative and costly designs.

One way to address this issue is to adjust the generation dispatch before the onset of an imminent natural disaster event. Here, the system operator can put in place a control strategy that proactively dispatches the system in anticipation that some sections/resources may become affected by the event and hence may become unavailable. Power grid operation subject to disturbances has been extensively addressed in the literature within the context of security-constrained optimal power flow (SCOPF) [4,5]. Here, the objective is to ensure that the system remains robust with respect to credible contingencies, and the system constraints are maintained should one of these contingencies happen. Traditionally, this was done through performing deterministic security assessment, where all contingencies are assumed to have equal probabilities of occurrence. This could create problems since it would emphasize on very severe events, making the solution overly conservative [6]. In order to incorporate the uncertain nature of disturbances, some have adopted stochastic approaches for solving the OPF and SCOPF problems. For instance, Yong and Lasseter [7] incorporated the expected value of reserve uncertainties into the objective function of the OPF. Minimizing the expected generation cost of various contingencies, in addition to the pre-contingency cost, has been reported in Ref. [8]. Multi-stage stochastic optimization

* Corresponding author. Tel.: +1 303 869 5040.
E-mail address: pjavanba@mymail.mines.edu (P. Javanbakht).

http://dx.doi.org/10.1016/j.epsr.2014.07.018
0378-7796/

Nomenclature

A. Indices

c	contingency index ($c=0$ for normal operating condition)
h	hurricane index
i	generator index
j	line index
k	bus index
l	hurricane eye location index ($l=0$ indicates landfall)
p	hurricane track (path) index
s	hurricane scenario index

B. General parameters

a_i, b_i, c_i	coefficients of the cost function for generator i
c^g	mode control parameter that determines preventive or corrective dispatch modes. $c^g=0$ for preventive dispatch, $0<c^g\leq 1$ for corrective dispatch
NB	number of buses
NC	number of contingencies
NG	number of generators
NL	number of lines
NL_c	number of lines in a contingency c
NP	number of hurricane tracks (paths)
NT	number of 2-h simulation time steps
$P_i^{G,\max}$	maximum permissible active power injection by generator i
$P_i^{G,\min}$	minimum permissible active power injection by generator i
$Q_i^{G,\max}$	maximum permissible reactive power injection by generator i
$Q_i^{G,\min}$	minimum permissible reactive power injection by generator i
$S_j^{\max}$	capacity (rating) of transmission line j
$V_k^{\max}$, $\theta_k^{\max}$	maximum permissible voltage magnitude and phase angle at bus k
$V_k^{\min}$, $\theta_k^{\min}$	minimum permissible voltage magnitude and phase angle at bus k
α	hurricane land decay factor
$\alpha^r, \alpha^l, \alpha^v$	cost function weighting coefficients
β	modeling factor specifying the hurricane boundary
$\rho_{j,c}$	soft upper limit on the percentage of transmission line j capacity (rating) that can be used under contingency c. If all the capacity can be used: $\rho_{j,c}=1$. This indicates a soft constraint on the flow of the transmission line which can be violated subject to a penalty.
$\rho_{j,c}^{\max}$	hard upper limit on the percentage of transmission line j capacity (rating) that can be used under contingency c (note: $\rho_{j,c}^{\max}\geq\rho_{j,c}$). This indicates a hard constraint on the flow of the transmission line which cannot be violated at any time.
$\theta_{k1,k2}^{\min/\max}$	minimum or maximum permissible phase angle between buses $k1$ and $k2$

C. Power system variables

$P_{i,c}^G$, $Q_{i,c}^G$	active and reactive power of generator i during contingency c ($c=0$ indicates normal operation)
Pr_c	probability of contingency c
S_j	apparent power flow through transmission line j
$V_{k,c}, \theta_{k,c}$	voltage magnitude and phase angle at bus k under contingency c
Y_c	admittance matrix of the network for contingency c
$Y_{kk',c}$	(k, k')-th entry of Y_c
$\delta_{j,c}^l$	overload severity variable for line j during contingency c
$\delta_{j,k}^v$	over/undervoltage severity variable for bus k during contingency c
$\theta_{k1,k2,c}$	phase angle between buses $k1$ and $k2$ during contingency c

D. Hurricane variables

$d_{\max}(j, h)$	maximum distance between transmission line j and the eye of hurricane h
$d_{\min}(j, h)$	minimum distance between transmission line j and the eye of hurricane h
out_j	event indicating the outage of transmission line j as a result of hurricanes
$\Delta P_{0,s}$	difference between the pressure at the hurricane eye location and the pressure at r_s for scenario s (in mb), for a hurricane at landfall
$\Delta P_{l,s}$	difference between the pressure at the hurricane eye location and pressure at r_s for scenario s (in mb), for a hurricane at eye location l
Pr_s	normalized probability of scenario s
r_s	hurricane size: the radius of the area affected by the hurricane (in nautical miles, nm)
r_{mw}	radius to maximum wind speed (in nautical miles, nm)
t	time elapsed after hurricane landfall (in h); $t=0$ indicates landfall
$\hat{w}_j$	expected value of the maximum wind speed to which transmission line j is exposed
$\hat{w}_{j,p}$	expected value of the maximum wind speed to which transmission line j is exposed if hurricane travels along track p
w_m	maximum sustained wind speed (in nautical miles per hour, kt)
$W(x)$	static wind field; as a function of distance to the hurricane eye
x	distance to the hurricane eye
x_0	hurricane eye location at landfall
v	hurricane translational speed
φ_t	latitude (in degrees) at time t
φ_l	latitude (in degrees) at eye location l
ψ_t	longitude (in degrees) at time t
ψ_l	longitude (in degrees) at eye location l

formulations have also been proposed [9,10], where event uncertainties are handled through the usage of second (or multi) stage recourse variables. At the same time, acknowledging the fact that inequality constraints in the OPF/SCOPF problem are not always rigid, and may be allowed to be slightly violated at times, some have used techniques based on chance constrained optimization [11,12], where inequality constraints are met with a certain probability. In a different approach, cumulant method was used to solve the uncertainties of the OPF problem [13].

However, in most of these approaches based on SCOPF, the exposure of the system to failure as a result of a contingency is either unknown or modeled subjectively. In fact, SCOPF does not differentiate between the contingencies with severe impacts on the system and those with minor impacts. Rather, it only ensures that there exists a low cost feasible solution satisfying all the contingencies as well as the normal operating condition, without considering the quality of that solution in terms of system security. To solve this issue, risk-based security assessment was proposed [6], where the notion of risk was modeled as a combination of severity of a

contingency and its probability of occurrence. This way, the risk index was defined as a measure of the system's exposure to failure. Li and McCalley proposed a general risk-based formulation for the SCOPF problem (RB-SCOPF) [14]. Similarly, a preventive DC RB-SCOPF was adopted in [15]. As opposed to SCOPF based approaches, RB-SCOPF attempts to provide a secure solution with less likelihood of exposure to failure by taking into consideration the severity as well as the likelihood of contingency events.

Although research on secure dispatch of the power grid and the incorporation of risk in the problem has been well established, fewer studies have been reported in the literature focusing on the impact of weather and natural disasters on power grid failure rate and outages (for example, see [16–19]). Even then, linking the mathematical formulation for secure grid dispatch to realistic natural disaster event scenarios is relatively unexplored. This is the focal point of the current paper.

In this paper, a risk-averse dispatch model is proposed based on AC SCOPF in order to provide power grid resiliency against hurricanes. The proposed model enables the power system operator to proactively dispatch the generation resources in the anticipation of an imminent hurricane. As such, this is a solution for operation time-frame that can be utilized during emergency conditions when the power grid is about to be affected by an incoming large-scale disturbance. To model the probability of multiple component outages, a geographical analysis is necessary that takes into account the locations of the transmission lines and buses as well as the path, size and wind field of the hurricane. Therefore, the IEEE 118-bus power grid is plotted onto the map of the state of Texas in order to provide realistic scenarios that are tied with historical data on hurricanes. However, the algorithm developed here is generic and can be applied to similar problems of the same nature.

2. Mathematical modeling of hurricanes

The first step for assessing the risks imposed by a hurricane on the power grid is to model the event mathematically. To achieve this goal, a statistical modeling approach is proposed here where each hurricane is modeled through its static and dynamic gradient wind fields. In the following, the details are presented.

2.1. Static gradient wind field

In general, the gradient wind field of a hurricane at any point in time can be given as a function of the distance to the eye, i.e. the hurricane center [20,21]. As a hurricane travels along its track, the field is portrayed as a vortex with translational movement. The static field is, in essence, the time snapshot of the hurricane wind field, whereas its time varying behavior is represented through the dynamic field. It is known that the field contour lines of a mature hurricane are concentric circles [21,22]. Inspired by the vortex shape of the static gradient wind field of Hurricane Katrina in 2005 [21], a function is proposed here to model the static wind field as shown in (1):

$$W(x) = \begin{cases} \xi(1 - \exp[-\psi x]) & 0 \le x < r_{mw} \\ w_m \exp\left[-\left(\dfrac{\ln\beta}{r_s - r_{mw}}\right)(x - r_{mw})\right] & r_{mw} \le x \le r_s \\ 0 & x > r_s \end{cases} \quad (1)$$

$$\xi = K \times w_m; \quad \psi = \frac{1}{r_{mw}} \ln\left(\frac{K}{K-1}\right), \quad K > 1$$

where w_m is 1-min average wind measured at about 10 m above the surface. The boundary of the hurricane is assumed to be a circle on which the wind speed has been reduced to w_m/β. Without loss of generality, it is assumed in this paper that the hurricane has no detrimental influence outside its outer boundary. As such, at any point in time, the hurricane is modeled by the parameter set $m = \{w_m, r_{mw}, r_s\}$.

The field contour lines are concentric circles with the values given in (1). The contour lines of the static wind field and the graph of function (1) are illustrated in Fig. 1a and b. Fig. 1c shows the comparative schematics of the gradient wind field of Hurricane Katrina at landfall [5] and the synthesized hurricane generated by (1) where $K = 1.14$ and $\beta = 10$. It was observed that as K gets closer to 1, the model provided more conservative estimates of the speeds.

2.2. Dynamic gradient wind field

The dynamic gradient wind field of a hurricane is a time-varying field with a translational movement and can be modeled as follows:

$$W_d = W(x|m(m_0, t, p, v_t, \alpha), \quad x_0(t, p, v_t)) \quad (2)$$

where m_0 represents the modeling parameter set of the hurricane at landfall. In essence, W_d is a generalized representation of the static field with time-varying modeling parameters and eye location.

2.3. Statistical analysis of hurricane parameters

In this section, statistical analysis of hurricane parameters $\{w_m, r_{mw}, r_s\}$ is provided based on the historical data of the US hurricanes (1851–2012) [23]. The main objectives are twofold: (*a*) determine the probability density function (PDF) of each parameter and (*b*) determine whether the parameters are dependent, independent or in general, correlated.

To address (*a*), it has been noted that in the literature, the normal and lognormal distribution functions are usually proposed for PDF of w_m and r_{mw}, respectively [21,22]. However, it was observed in the simulations that after landfall, the PDF of each parameter changes shapes as the hurricane travels inland. Therefore, the kernel density estimation (KDE) is adopted here to derive the PDFs of the hurricane parameters, due to its non-parametric nature that suits various applications.

To address (*b*), mutual scatter plots of the hurricane parameters are analyzed for the past US hurricanes with intensities 3, 4 and 5 based on the Saffir-Simpson scale [24], as these intensity categories are assumed to be most detrimental to the power grid. The results are shown in Fig. 2 where individual KDEs and mutual scatter plots are illustrated in parts (a)–(c) and parts (d)–(f), respectively. According to the plots, no linear correlation between the parameters can be observed. This confirms that the parameters can be sampled independently using the associated KDEs and grouped together to create hurricane samples for simulation.

Assuming forecast information on the hurricane tracks is available through the national hurricane center [25], and further considering the translational speed of the hurricane to be constant, an algorithm is proposed here to model the dynamic wind field of the hurricane (2) as it moves along a track. Here, without loss of generality, the eye locations are specified every two hours for a total duration of twelve hours:

1. Assume a landfall location (φ_0, ψ_0), NP equally probable tracks and NT 2-h simulation time steps.
2. Given the forecasted track data and hurricane translational speed, use data in step 1 to calculate the hurricane eye locations at each point in time, i.e. (φ_t, ψ_t).
3. Simulate N_0 hurricanes at landfall as stated previously.

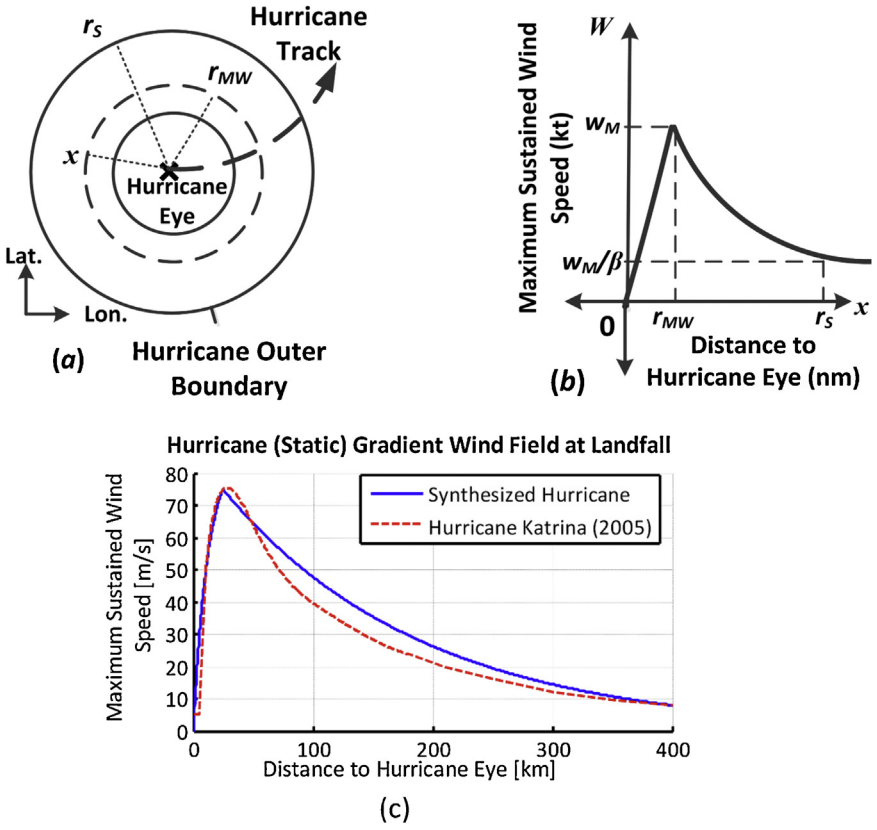

Fig. 1. Static gradient wind field: (a) 2D snapshot of the contour lines of maximum sustained wind speeds at any point in time, (b) synthesized static gradient wind field of hurricane, (c) comparative illustration of the gradient wind fields of Hurricane Katrina and its synthetic model.

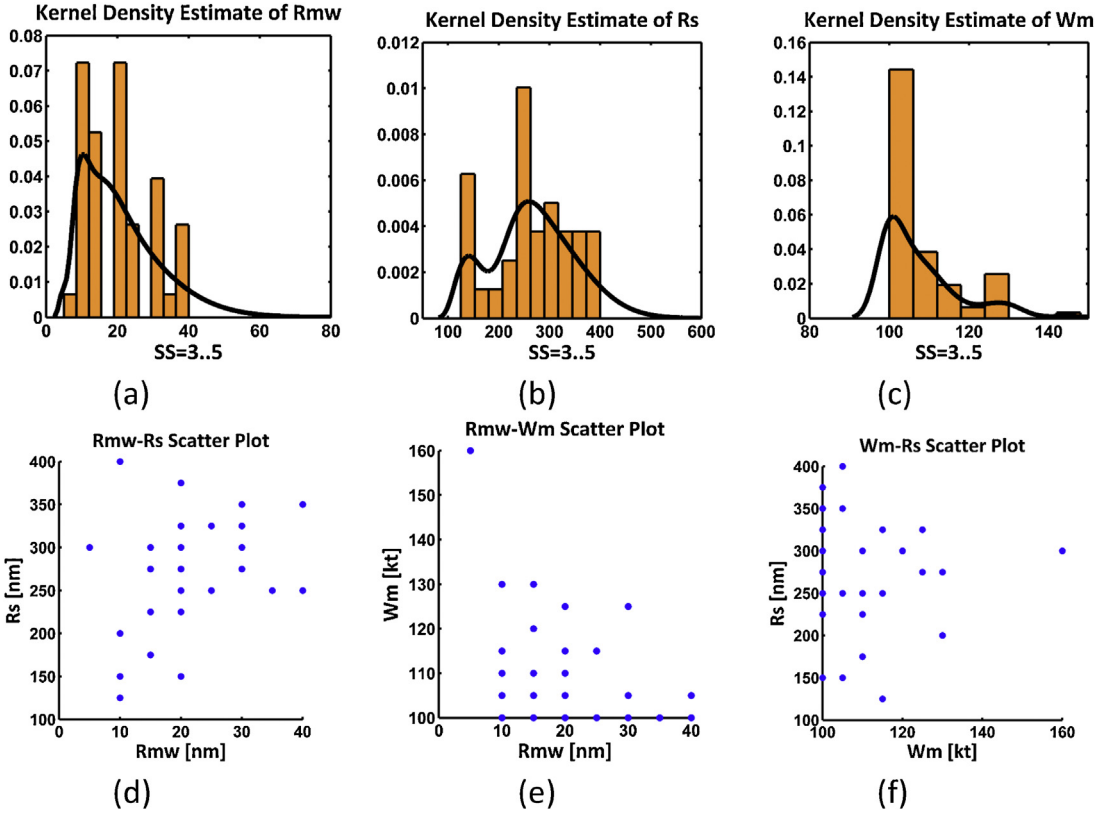

Fig. 2. Illustrative results of statistical analysis of hurricane parameters in the US: (a)–(c): KDE of parameters: Rmw and Rs in nautical miles (nm), and Wm in nautical miles per hour (kt) (d)–(f): mutual scatter plots of the parameters. Each dot represents a hurricane observation. SS = Saffir-Simpson scale.

4. Take N_0 samples of a lognormal PDF with parameters $\mu = -3.466$ and $\sigma = 0.703$ (for the state of Texas [21]) to simulate the land decay factor α.
5. Scenario index $s \leftarrow 1$.
6. Extract $m_{0,s} = \{w_{m0,s}, r_{mw0,s}, r_{s0,s}\}$ from step 3.
7. Calculate $\Delta P_{0,s}$ (mb) at landfall using (3) [21]:

$$\Delta P_{0,s} = \sqrt{\frac{2.636 + 0.0394899 \times \varphi_0 - \ln(r_{mw0,s})}{0.0005086}} \quad [\text{mb}] \tag{3}$$

8. Calculate Holland pressure parameter B at landfall, i.e. $B_{0,s}$, using (4) [21]:

$$B_{0,s} = 1.38 + 0.00184\Delta P_{0,s} - 0.00309 r_{mw0,s} \tag{4}$$

9. Calculate $\Delta P_{l,s}$ at eye location l (at time t_l after landfall; can be on each track p) for each specific land decay factor in step 4 based on the filling model proposed in [21]:

$$\Delta P_{l,s} = \Delta P_{0,s} \times \exp[-\alpha_s \times t_l] \tag{5}$$

where $l = 1, 2 \ldots NP \times NT$ is the index of each eye.
10. Using the eye locations (φ_l, ψ_l), calculate radius to maximum winds for the traveling hurricanes at eye location l as follows [22]:

$$r_{mw_l,s} = \exp[2.636 - 0.0005086\Delta P_{l,s}^2 + 0.0394899\varphi_l] \tag{6}$$

11. Calculate Holland pressure parameter B using (5) and (6) at each location as follows:

$$B_{l,s} = 1.38 + 0.00184\Delta P_{l,s} - 0.00309 r_{mw_l,s} \tag{7}$$

12. Calculate w_m at each eye location on the track as follows [22]:

$$w_{m_l,s} = w_{m0,s}\sqrt{\frac{B_{l,s} \times \Delta P_{l,s}}{B_{0,s} \times \Delta P_{0,s}}} \tag{8}$$

13. As there is no evident correlation between r_S and the other two parameters, take $NP \times NT$ simple random samples (SRSs) of r_s using its PDF and finalize the simulation of hurricane parameters by pairing these with all the simulated parameters.
14. While $s < N_0$, $s \leftarrow s + 1$ and repeat steps 6–13 for each hurricane at landfall.

In order to assure the validity of step 13, it is necessary to verify that the sizes of hurricanes with different intensities can be used interchangeably. Two hypothesis tests are performed in this regard, namely: (*a*) two-sided χ^2 variance test to compare the variances of the two populations (equal is the null hypothesis and unequal is the alternative) and (*b*) two-sided *t*-test to compare the difference in means of two populations (zero is the null hypothesis and non-zero is the alternative). The populations are hurricanes of two different intensities and the test statistic is the hurricane size. The results for 95% confidence level are summarized in Table 1 based on which it can be concluded that we are 95% confident that when the intensity of a hurricane is larger than three, there is insignificant difference in the sizes of hurricanes with different intensities.

In a more detailed analysis, the algorithm may require a methodology for determining the sample size (N_0). However, this aspect is considered to be outside the scope of the present study. Therefore, a predetermined value (i.e. $N_0 = 7000$) is adopted. Landfall location was considered to be the coastline of the state Texas (i.e. $\varphi_0 = 28.9^\circ$N, $\psi_0 = 95.2^\circ$W). The hurricanes generated based on the methodology proposed in this section will then be used to assess the hurricane-induced risks on the power grid.

3. Hurricane effects on the power grid

Although different power grid components may be affected by hurricanes, the focus of this paper is on transmission lines. In order to assess the risk imposed on the power grid due to high wind speeds of a hurricane, it is necessary to calculate the probabilities of line outages due to various hurricane scenarios. A methodology is proposed in this section that provides the probabilities for the (N–k) contingency analysis based on the simulated hurricanes.

3.1. Hurricane impact matrix

The hurricane impact matrix, denoted as "HIM", provides the maximum sustained wind speed that each transmission line would get exposed to under each hurricane scenario, and is defined as follows:

$$him_{j,h} = \begin{cases} w_{m_h} & d_{\min}(j,h) \le r_{mw_h} \le d_{\max}(j,h) \\ \max\begin{pmatrix} W_{d_h}(d_{\min}(j,h)|m_h) \\ W_{d_h}(d_{\max}(j,h)|m_h) \end{pmatrix} & \text{otherwise} \end{cases} \tag{9}$$

where m_h is the modeling parameter of hurricane h.

In this paper, transmission lines are treated as objects of multiple segments where the distance between each line and a specific hurricane is calculated based on the minimum distance of each segment and the hurricane eye. Here, it is assumed that if a hurricane hits one point along the line, the whole line is considered affected. Clearly, $him_{j,h} = 0$ indicates that all segments of line j are out of the outer boundary of hurricane h.

3.2. Outage probabilities

In order to calculate the outage probabilities, the affected objects of the grid are first detected based on the hurricanes simulated for each track. Then, the wind speed PDFs of the affected objects are non-parametrically estimated using KDE (using the data from the HIM matrix). As a result, for each affected component, NP PDFs are achieved. Depending on the type of the object, different formulations can be adopted. Here, it is assumed that the outage probability of a transmission line depends on the expected value of the wind speed $\hat{w}_j$ to which the line is exposed as shown in (10):

$$\Pr\{\text{out}_j\} = \begin{cases} 0 & \hat{w}_j \le w_1 \\ \dfrac{\hat{w}_j - w_1}{w_2 - w_1} & w_1 \le \hat{w}_j \le w_2 \\ 1 & \hat{w}_j \ge w_2 \end{cases} \tag{10}$$

where w_1 and w_2 are constant wind speeds which may lead to the line outage (here without loss of generality: $w_1 = 110$ mph and $w_2 = 155$ mph). The value $\hat{w}_j$ is calculated based on the PDF of the wind speeds affecting the transmission line j:

$$\hat{w}_j = \sum_{p=1}^{Np} \Pr_p \cdot \hat{w}_{j,p} = \sum_{p=1}^{Np} \Pr_p \int_0^\infty u \times f_{j,p}(u)du \tag{11}$$

In (11), $\Pr_p$ is the probability of hurricane traveling along track p, and f indicates the PDF of the hurricane speeds experienced by line j. This PDF is developed based on the hurricane samples created in the previous section. The flowchart of the algorithm proposed here to calculate the outage probabilities is shown in Fig. 3.

3.3. Contingency probabilities

The probability of different (N–k) contingencies now need to be calculated based on the individual line outage probabilities calculated in the previous section. In order to achieve this, a clustering algorithm is adopted in this section as follows:

Table 1
Results of hypothesis tests.

SS_A	SS_B	χ^2 variance test results ($\alpha = 0.05$)		T-test results ($\alpha = 0.05$)	
		Null hypothesis	p-Value	Null hypothesis	p-Value
1	2	Failed to reject	0.6381	Rejected	0.0248
1	3	Failed to reject	0.5303	Rejected	0.0082
1	4	Failed to reject	0.5979	Failed to reject	0.4125
2	3	Failed to reject	0.3456	Failed to reject	0.7463
2	4	Failed to reject	0.8376	Failed to reject	0.5323
3	4	Failed to reject	0.3711	Failed to reject	0.3456

1. Find the similarity/dissimilarity between each pair of the affected objects using a distance matrix whose entries are the Euclidean distances among the outage probabilities.
2. Using the distance matrix, group the pairs that are in close proximity. Note that within this context, proximity is defined as the closeness in the value of the outage probabilities for individual hurricanes. In this stage, a cluster tree is made.
3. Combine the clusters whose distances are less than a certain threshold into larger clusters. This way, the objects (lines) which in a similar fashion are exposed to hurricanes are grouped together. Each cluster realizes an (N–k) contingency. It should be noted that the probability of each contingency is different from the individual outage probabilities of the enclosed objects.

The final number of clusters is an important parameter that depends on the relative consistency of each link in the hierarchical cluster tree. This can be quantified through the inconsistency coefficient which compares the height of a link in a cluster hierarchy with the average height of the links below it.

Note that in the calculation of these contingency probabilities, it has been assumed that the hurricane has in fact occurred. Because of this, the probabilities are denoted here as Pr(c|hurricane) and are essentially the arithmetic average of the outage probabilities of the lines (components) included into the same cluster. These probabilities are then modified and used in the generation dispatch model (as described in Section 4).

4. Proposed RB-SCOPF methodology

The ultimate objective of this study is to proactively modify the generation dispatch of a power system with the goal of minimizing the generation cost and at the same time, the hurricane-induced cumulative risk of outage. For this, (N–k) contingency analysis has been performed that considers the probabilities of line outages due to hurricanes. In addition, both over/undervoltage and line overload risks are included making the dispatch model a risk-averse type. In this section, based on the hurricane scenarios and the associated line outage probabilities presented in the preceding sections, a RB-SCOPF is formulated to minimize the impacts and costs caused by

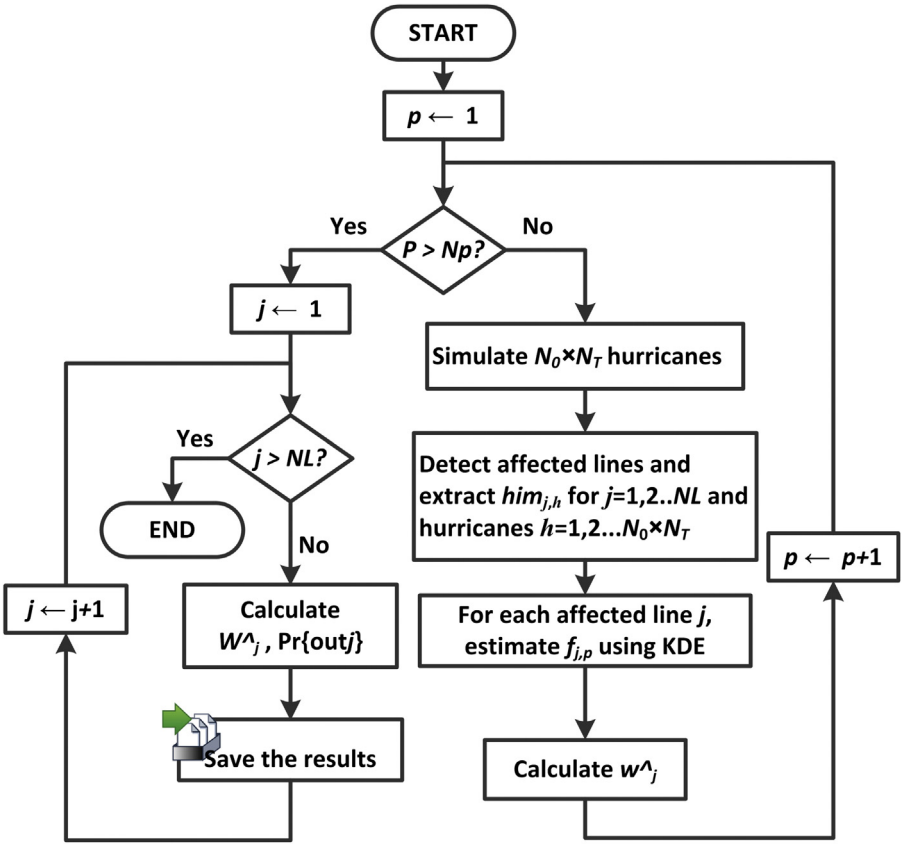

Fig. 3. Flowchart of outage probability calculation algorithm.

hurricanes on the power grid. The proposed RB-SCOPF problem is formulated as follows:

$$\text{Min} \sum_{i=1}^{NG} (a_i (P_{i,0}^G)^2 + b_i P_{i,0}^G + c_i) + \alpha^r \sum_{c=0}^{NC} \text{Pr}_c \left\{ \sum_{j=1}^{NL_c} \alpha^l \delta_{j,c}^l + \sum_{k=1}^{NB} \alpha^v \delta_{k,c}^v \right\} \quad (12)$$

The objective function (12) consists of two terms: (*a*) the generation cost (first term), (*b*) the risk cost (second term), which comprises overload and over/undervoltage risks. It is assumed here that the overload and over/undervoltage costs increase linearly as per-unit loading of each line or per-unit voltage of each bus exceeds the permitted ranges.

The optimization problem is solved subject to (13)–(23):

- *Load flow constraints*: this is the set of the equality constraints that reflect the AC power flow equations. In vector form, this can be represented as (13):

$$\forall i, \forall c : P_{i,c}^G - jQ_{i,c}^G = V_{k,c}^* \sum_{k'=1}^{NB} Y_{kk',c} V_{k',c} \quad (13)$$

- *Line flow constraints*: during normal operating condition, the flow of the line has to be less than the maximum rated value. However, during different contingencies, this may not at times be possible. Most utilities allow for temporary violation of their line rating during emergency conditions [26]. In the formulation proposed here, it is assumed that for a line j this upper limit can be temporarily relaxed under contingency c by the ratio of $\delta_{j,c}^l$ (to be determined by the optimization problem).

$$\forall j, \forall c : S_{j,c}(V_c, \Theta_c, Y_c) \le (\rho_{j,c} + \delta_{j,c}^l) \cdot S_j^{\max} \quad (14)$$

- *Voltage security constraint*: during normal operating condition, bus voltages must lie within the permissible range provided by ANSI. However, during different contingencies, this may not at times be possible. In the formulation proposed here, it is assumed that for a bus k this range can be temporarily relaxed under contingency c by the ratio of $\delta_{k,c}^v$ (to be determined by the optimization problem).

$$\forall k, \forall c : (1 - \delta_{k,c}^v) \cdot V_k^{\text{avg}} \le V_{k,c} \le (1 + \delta_{k,c}^v) \cdot V_k^{\text{avg}}$$
$$V_k^{\text{avg}} = \frac{V_k^{\min} + V_k^{\max}}{2} \quad (15)$$

- *Preventive/corrective dispatch constraint*: in the power system, control actions can be classified into two categories: corrective and preventive [27]. Preventive remedial decisions are made before the onset of a contingency and do not allow any change of the control variables in post-contingency states. In other words, active and reactive powers of generators, tap ratios, shunt reactors, and load apparent powers have to remain fixed. Corrective decisions, however, are made more based on economic objectives than security, as they allow rescheduling the control variables up to a certain limit. The proposed formulation allows for preventive versus corrective dispatch. In the latter case, the amount by which the outputs of the generators can change with respect to the normal operating condition can be limited. Note that the mode control parameter c^g in general can have different values for each generator and in each contingency.

$$\forall i, \forall c : (1 - c_{i,c}^g) \cdot P_{i,0}^G \le P_{i,c}^G \le (1 + c_{i,c}^g) \cdot P_{i,0}^G \quad (16)$$

- *Upper and lower bound constraints*:

$$\forall i, \forall c : P_i^{G,\min} \le P_{i,c}^G \le P_i^{G,\max} \quad (17)$$

$$\forall i, \forall c : Q_i^{G,\min} \le Q_{i,c}^G \le Q_i^{G,\max} \quad (18)$$

$$\forall k, \forall c : V_k^{\min} \le V_{k,c} \le V_k^{\max} \quad (19)$$

$$\forall k, \forall c : \theta_k^{\min} \le \theta_{k,c} \le \theta_k^{\max} \quad (20)$$

- *Constraints on overload and over/undervoltage severity variables*: these are limits put in place to control the range of severity variables that help relax overload and over/undervoltage constraints. These constraints assist in discarding solutions that tend to be technically undesirable.

$$\forall k, \forall c : 0 \le \delta_{k,c}^v \le \frac{V_k^{\max} - V_k^{\min}}{2} \quad (21)$$

$$\forall j, \forall c : 0 \le \delta_{j,c}^l \le \rho_{j,c}^{\max} - \rho_{j,c} \quad (22)$$

- *Dynamic bus angle constraints*: the limit on line angle is especially important in line switching and FACTS applications, and represents a concept different from line loading. Although this paper focuses on steady state operation, a limit is enforced on the differences between phase angles of buses connected to one another during contingencies so that the results are also appropriate when operated in transient and dynamic states.

$$\forall k1, k1 \in \{1, \ldots, NB\}, \forall c : \theta_{k1,k2}^{\min} \le \theta_{k1,k2,c} \le \theta_{k1,k2}^{\max}$$
$$\theta_{k1,k2,c} = \theta_{k1,c} - \theta_{k2,c} \quad (23)$$

To calculate the probability of each contingency (Pr_c) the following assumption has been made: An imminent event will occur after T_1 units of time with a certainty factor CF (e.g. we are 90% confident that a hurricane will make landfall within the next T_1 hours, then CF = 0.90). Assume that the system operator desires a proactive generation dispatch that maintains the system until T_2 units of time after the event (i.e. hurricane landfall). As a result, the dispatch interval $T_D = T_1 + T_2$ is defined as the time during which the generation dispatch remains valid. Based on these assumptions, Pr_c is calculated as in (24), where Pr(*c*|hurricane) is calculated based on the algorithm in Section 3.3:

$$Pr_c = \begin{cases} \frac{T_2}{T_D}(1 - CF) + \frac{T_1}{T_D} & c = 0 \\ \frac{T_2}{T_D} CF \cdot \text{Pr}(c|\text{hurricane}) & c \ge 1 \end{cases} \quad (24)$$

The complete hurricane risk-averse dispatch model (12)–(23) is solved using a MATLAB-based interior point solver for OPF using the MATPOWER software [28].

5. Numerical results

The numerical results are presented in two parts. First, the IEEE 118-bus power system is fitted onto the map of the state Texas. This geographical zone is selected for demonstration purposes only. The historical data in [23,25] have been used for simulation. Although historical data have been applied for producing the hurricane database, the simulated hurricanes do not refer to any actual events. It is often safe to assume that the hurricane landfall and possible inland pathways can be forecasted by US National Hurricane Center with relative accuracy (see [25] for past examples). These parameters are therefore assumed known. A Monte-Carlo simulation study is then performed based on the proposed 14-step algorithm of Section 2.2. This provides the geographic information about the simulated hurricanes comprising latitude and longitude of the hurricane eye locations, radius to maximum wind speed of hurricane and its wind field. Using this information, together with the geographic data of the power grid, i.e. IEEE 118-bus, the line outage probabilities are calculated using (9)–(11). Then, based on the outage probabilities and the clustering algorithm mentioned in Section 3.3, the (*N*–*k*) contingency scenarios are generated based on which, the dispatch model (12)–(23) is solved.

Table 2
Preliminary hurricane data: landfall ($\varphi 0 = 28.9^\circ$N, $\psi 0 = 95.2^\circ$W).

Track (1)	Track information: length = 108 miles, azimuth = 340°						
	Eyes	1	2	3	4	5	6
	φ (°N)	29.14	29.39	29.63	29.88	30.12	30.37
	ψ (°W)	95.30	95.40	95.51	95.61	95.71	95.82
Track (2)	Track information: length = 108 miles, azimuth = 330°						
	Eyes	1	2	3	4	5	6
	φ (°N)	29.13	29.35	29.58	29.80	0.03	30.25
	ψ (°W)	95.35	95.50	95.65	95.80	95.95	95.10
Track (3)	Track information: length = 108 miles, azimuth = 320°						
	Eyes	1	2	3	4	5	6
	φ (°N)	29.10	29.30	29.50	29.70	29.89	30.09
	ψ (°W)	95.39	95.58	95.78	95.97	96.17	96.36

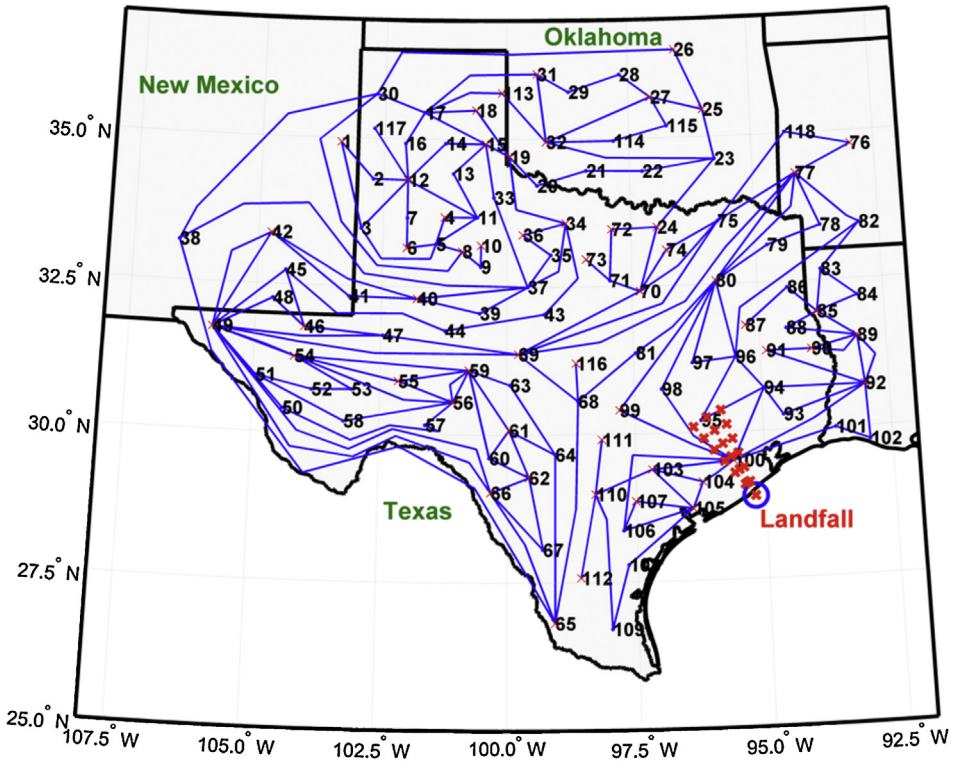

Fig. 4. Mapping of the IEEE 118-bus grid onto the map of the state of Texas, illustrating the example hurricane tracks.

5.1. Hurricane simulation

A landfall location and three equally probable tracks given in Table 2 are assumed known for the hurricanes. The reader should note that, in the general case, the probabilities of different tracks could be different. However, for simplicity, they are assumed to be equal here.

Fig. 4 illustrates the power grid mapped onto the map of the state of Texas, as well as the forecasted tracks (used for demonstration purposes in the case study). The electrical data of the test system is provided in Ref. [29]. The hurricanes are assumed to be slow moving with a translational speed of 9 mph. The hurricanes are simulated assuming they travel inland for 12 h (i.e. $T_2 = 12$ h); therefore, six 2-h time-steps are studied. Moreover, without loss of generality, it is assumed here that hurricanes with intensities $SS \geq 3$ (i.e. with maximum wind speeds $w_m \geq 96$[kt]) take place at landfall. By taking into consideration the historical observations, the PDF of each parameter of hurricane is estimated non-parametrically where eventually, 7000 samples of hurricanes are generated at landfall. Finally, the parameters of hurricanes at each eye location

Table 3
Outage and contingency probabilities.

Cluster index	Transmission line outages (from bus, to bus,)	Pr (c|hurricane)	
1	(92, 100), (98, 100), (99, 100), (100, 106)	0.487	
2	(94, 100), (100, 101), (100, 103), (100, 104)	0.421	
3	(103, 104), (103, 105)	0.092	
Contingency probabilities			
Pr_0	Pr_1	Pr_2	Pr_3
0.4	0.2922	0.2526	0.0552

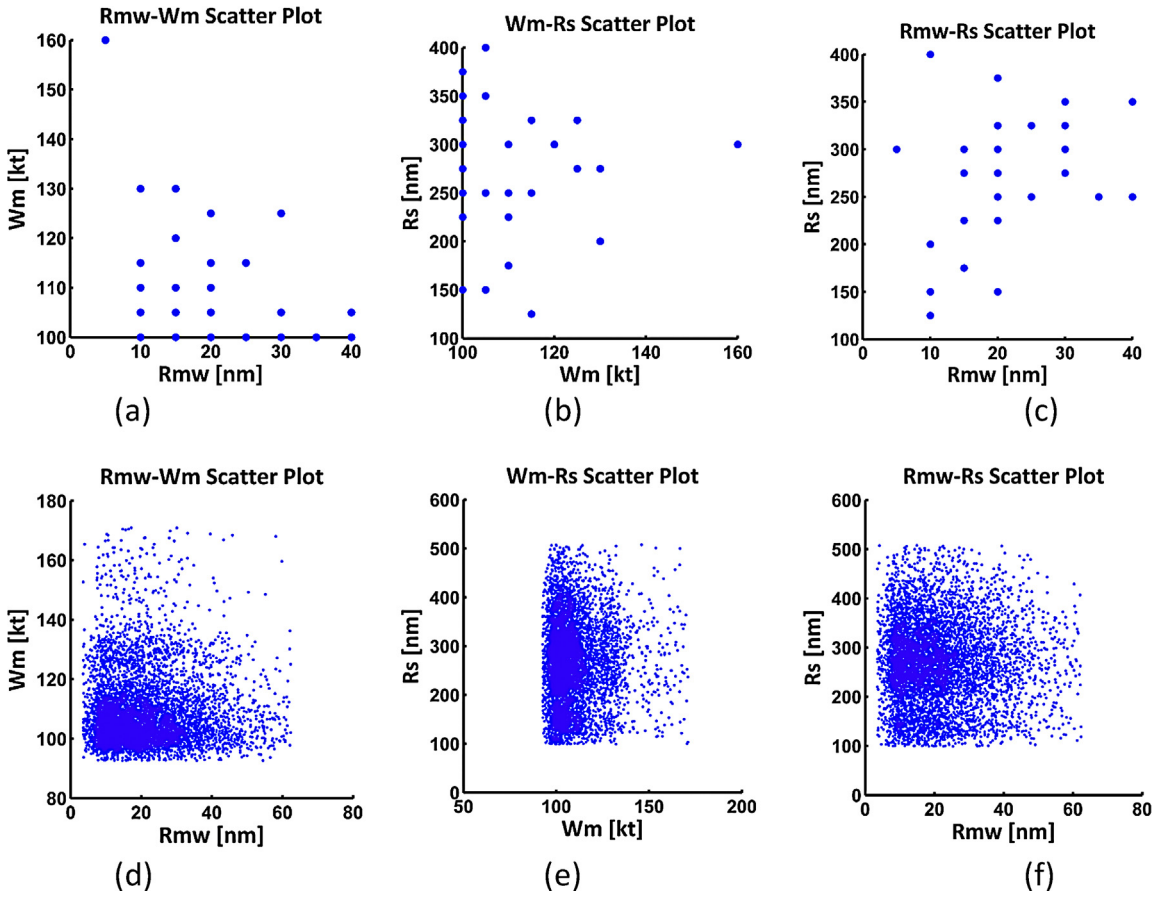

Fig. 5. Comparative scatter plots of hurricane parameters: (a)–(c) historical observations of US hurricanes, (d)–(f) simulated hurricanes.

on the tracks are computed deterministically as hurricanes travel inland. The comparative scatter plots of the parameters of actual as well as simulated hurricanes at landfall are illustrated in Fig. 5 where each point represents a hurricane.

5.2. Power system simulation results

Considering the simulated hurricanes and geographic data of the grid, three multi-contingency scenarios are extracted here based on the "*HIM*" matrix and the outage probabilities. The steps taken are as follows:

(a) a list of the affected lines and their outage probabilities are extracted,
(b) the mutual Euclidean distances of the outage probabilities are calculated,
(c) affected lines with minimum distances are paired up,
(d) using the statistics toolbox of MATLAB, a binary cluster tree (dendrogram) is built illustrating the distances between different pairs and potential clusters,
(e) using this tree, a suitable number of scenarios is specified providing the most consistent clustering,
(f) finally, the clusters and their average outage probabilities are extracted. The dendrogram is shown in Fig. 6.

Assuming CF = 0.9, the final results of the scenarios including the scenario index, affected lines and probabilities are given in Table 3 based on which the dispatch model (13)–(23) is solved.

To solve the RB-SCOPF, it is assumed that a hurricane is forecasted to make landfall within the next 6 h (T_1 = 6 h), which will

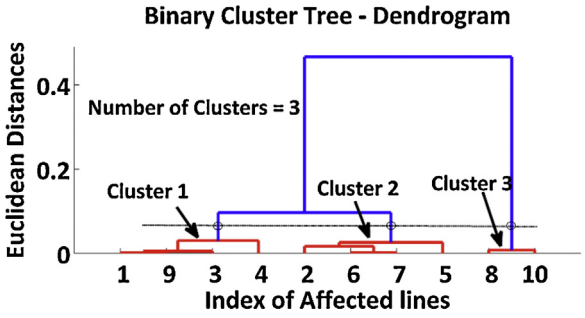

Fig. 6. The binary cluster tree (dendrogram) for cluster analysis.

continue moving inland for 12 h (T_2 = 12 h). This way, the total dispatch time T_D is 18 h.

Power grid dispatch problem has been solved for three types of problems, namely, (a) the classical AC OPF where all the scenarios and risk related variables are ignored in the objective function (12), (b) Risk-Based OPF (RBOPF) where the contingency scenarios are all ignored and only the risk variables are added to the AC OPF, and finally, (c) the Risk-Based Security Constrained OPF (RB-SCOPF) where (12) is fully formulated. The data used are provided in Table 4.

Table 4
Parameters of the dispatch model.

ρ	V^{max}	V^{min}	ρ^{max}	α^r	c^g	α^l	α^v
0.9	1.05	0.95	1.2	1	0.1	10^4	10^4

Table 5
Comparative simulation results.

	AC OPF	RB-OPF	RB-SCOPF		
			$c^g = 0.56$	$c^g = 0.1$	$c^g = 0.01$
Generation cost ($)	129.660	130.330	130.350	130.360	130.364
Tot. power loss (MW)	77.40	77.88	81.65	81.67	81.77
Mean (δ^l)		6.6×10^{-9}	4.5×10^{-13}	8.1×10^{-13}	4.6×10^{-13}
Mean (δ^v)		0.0054	0.0069	0.0069	0.0069
Min ($\|V\|$)	1.01 p.u	0.976 p.u	0.963 p.u	0.963 p.u	0.963 p.u
Max ($\|V\|$)	1.06 p.u	1.03 p.u	1.04 p.u	1.04 p.u	1.04 p.u
Iterations	19	19	22	22	23

Table 5 summarizes the results for three values of the preventive–corrective control gain c^g. It provides a comparison of the generation cost, total active power loss, the extreme values of bus voltages, the average values of voltage and overload risk variables, and the number of iterations of the optimization process for each value. The results show that as risk and security are incorporated into the dispatch problem, the generation cost increases. This is expected since the dispatch solution moves further away

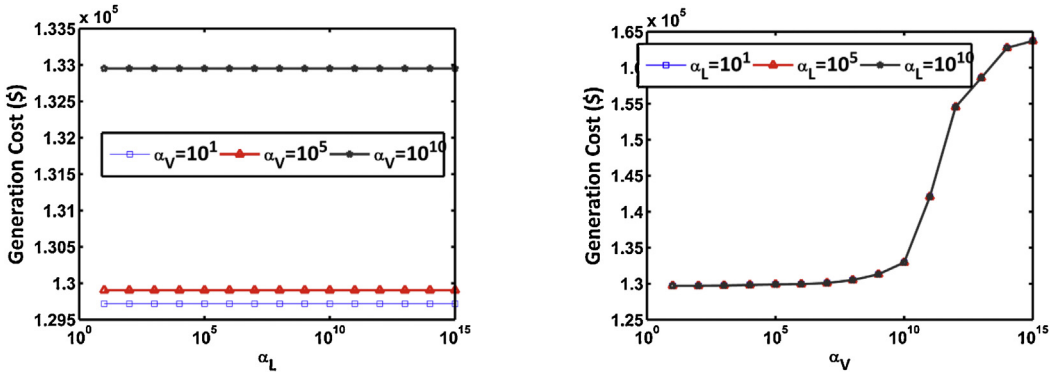

(a) Effect of risk coefficients on generation cost

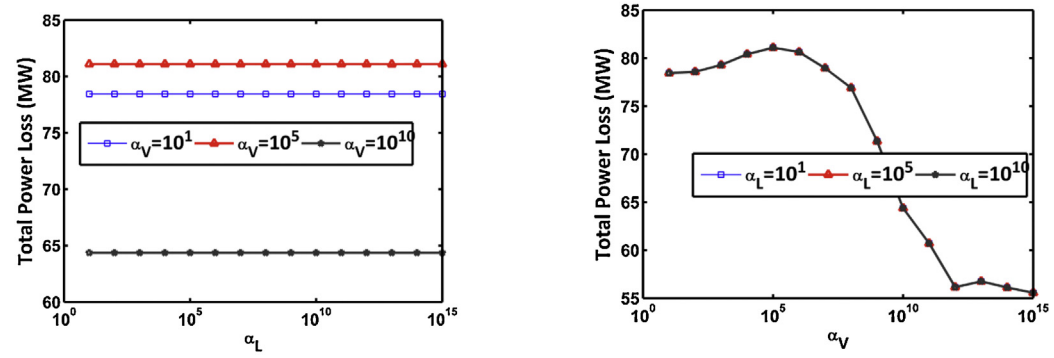

(b) Effect of risk coefficients on total power losses in the system

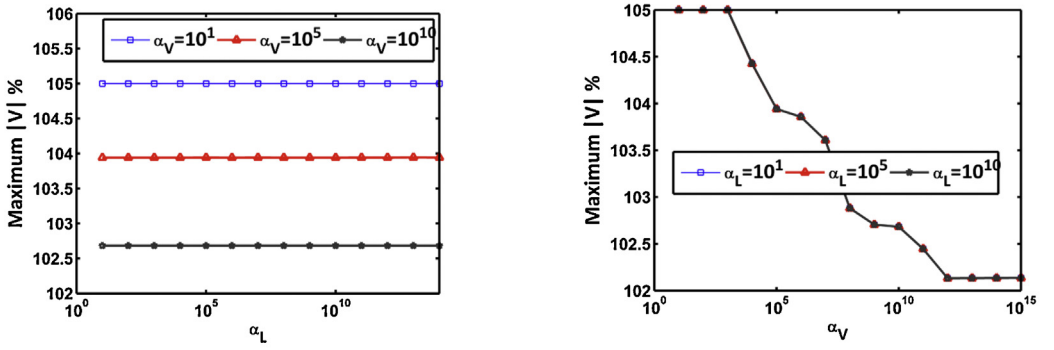

(c) Effect of risk coefficients on maximum node voltage across the network

Fig. 7. Variations of different network quantities with respect to risk coefficients α^l and α^v for RB-OPF (without contingencies).

from the financially optimal point. This comparison is beneficial for the system operator in deciding whether or not to incorporate the security constraints and the risk indices in the dispatch optimization problem.

It is also shown in Table 5 that as corrective dispatch turns into a preventive one (by reducing c^g to 0), the generation cost increases. This is natural, since corrective dispatch offers more flexibility at the hands of the system operator to steer the system toward a more economically viable point through the "wait and see" approach. However, under the preventative scheme, the system has to prepare itself for all possible contingencies by making the "here and now" decisions.

Another aspect which is important for the applicability of the proposed algorithm for real-time applications is the convergence speed. It was observed in the simulations that incorporating risk and security into the problem formulation increases the number of iterations needed to converge.

In addition, the effect of selecting different risk coefficients (α^l and α^v) on the network quantities has been investigated through the RB-OPF problem and the results are provided in Fig. 7. For each test, one coefficient is varied while the other is kept constant, and the effect of these variations on some network quantities has been shown. It can be seen that the over/undervoltage risk coefficient (α^v) has a more dominant effect on the network quantities than the overload risk coefficient of the lines (α^l). Of course, this is not necessarily a general rule, and can in fact be a characteristic of the system under study which is likely to be more vulnerable with respect to risk of over/undervoltage than the risk of line overload. It can be seen that higher values of α^v ensure that the maximum node voltage across the system reduces (likewise, minimum node voltage increases; not shown in the figure), which in turn leads to a reduction in power losses due to a flatter voltage profile. In general, for any system under study this sensitivity analysis has to be performed in order to select the right set of parameters.

6. Conclusion

A risk-averse generation dispatch methodology was proposed in this paper based on SC-OPF for a power grid subject to an imminent natural disaster event. The proposed algorithm provides means for preventive and/or corrective dispatch of the power system, and considers both operational costs as well as risks of overload and over/undervoltage. This solution is meant to assist a system operator in proactively dispatching the power grid in the event of a forthcoming hurricane.

Using available historical data on hurricanes at landfall, a detailed statistical analysis was performed to model hurricane parameters. These parameters were then used to simulate hurricane events. An algorithm was then developed to perform (N–k) contingency analysis based on the outage probabilities of transmission lines due to individual simulated hurricanes.

To provide a realistic test bed, the overall methodology was tested on the IEEE 118-bus power system mapped onto the map of the state of Texas. This geographical modeling allowed the usage of historical hurricane data available for the state of Texas. Parametric studies were carried out to investigate and show the importance of selecting suitable model coefficients.

References

[1] P. Hines, J. Apt, S. Talukdar, Large blackouts in North America: historical trends and policy implications, Energy Policy 37 (2009) 5249–5259.
[2] A. Kwasinski, W.W. Weaver, P.L. Chapman, P.T. Krein, Telecommunications power plant damage assessment for Hurricane Katrina – site survey and follow-up results, IEEE Syst. J. 3 (November (3)) (2009) 277–287.
[3] L.E. Link, The anatomy of a disaster, an overview of Hurricane Katrina and New Orleans, Ocean Eng. 37 (2010) 4–12.
[4] F. Capitanescu, J.L. Martinez Ramos, P. Panciatici, D. Kirschen, A. Marano Marcolini, L. Platbrood, L. Wehenkel, State-of-the-art, challenges, and future trends in security-constrained optimal power flow, Electr. Power Syst. Res. 81 (8) (2011) 1731–1741.
[5] B. Stott, O. Alsac, A.J. Monticelli, Security analysis and optimization, Proc. IEEE 75 (December (12)) (1987) 1623–1645.
[6] J.D. McCalley, V. Vittal, N. Abi-Sarma, An overview of risk based security assessment, in: Proc. IEEE PES Summer Meeting, Edmonton, Alberta, Canada, 1999, pp. 173–178.
[7] T. Yong, R.H. Lasseter, Stochastic optimal power flow: formulation and solution, in: Proc. IEEE PES Summer Meeting, Seattle, WA, USA, 2000, pp. 237–242.
[8] J. Condren, T.W. Gedra, Expected-security-cost optimal power flow with small signal stability constraints, IEEE Trans. Power Syst. 21 (4) (2006) 1736–1743.
[9] A. Rabiee, A. Soroudi, Stochastic multiperiod OPF model of power systems with HVDC-connected intermittent wind power generation, IEEE Trans. Power Deliv. 29 (1) (2014) 336–344.
[10] C.E. Murillo-Sánchez, R.D. Zimmerman, C.L. Anderson, R.J. Thomas, A stochastic contingency-based security constrained optimal power flow for the procurement of energy and distributed reserve, Decis. Support Syst. 56 (December) (2013) 1–10.
[11] H. Zhang, P. Li, Chance constrained programming for optimal power flow under uncertainty, IEEE Trans. Power Syst. 26 (November (4)) (2011) 2417–2424.
[12] M. Perninge, C. Hamon, A stochastic optimal power flow problem with stability constraints – Part II. The optimization problem, IEEE Trans. Power Syst. 28 (May (2)) (2013) 1849–1857.
[13] A. Tamtum, A. Schellenberg, W. Rosehart, Enhancements to the cumulant method for probabilistic optimal power flow studies, IEEE Trans. Power Syst. 24 (November (4)) (2009) 1739–1746.
[14] Y. Li, J.D. McCalley, Risk-based optimal power flow and system operation state, in: Proc. IEEE PES General Meeting, Calgary, AB, Canada, July, 2009.
[15] Q. Wang, J.D. McCalley, T. Zheng, E. Litvinov, A computational strategy to solve preventive risk-based security-constrained OPF, IEEE Trans. Power Syst. 28 (2) (2013) 1666–1675.
[16] H. Liu, R.A. Davidson, T.V. Apanasovich, Spatial generalized linear mixed models of electric power outages due to hurricanes and ice storms, Reliab. Eng. Syst. Saf. 93 (2008) 875–890.
[17] Y. Zhou, A. Pahwa, S.S. Yang, Modeling weather-related failures of overhead distribution lines, IEEE Trans. Power Syst. 21 (4) (2006) 1683–1690.
[18] A. Shafieezadeh, U.P. Onyewuchi, M.M. Begovic, R. DesRoches, Age-dependent fragility models of utility wood poles in power distribution networks against extreme wind hazards, IEEE Trans. Power Deliv. 29 (February (1)) (2014) 131–139.
[19] A. Castillo, Risk analysis and management in power outage and restoration: a literature survey, Electr. Power Syst. Res. 107 (2014) 9–15.
[20] B.A. Williams, D.G. Long, Estimation of hurricane winds from seawinds at ultra-high resolution, IEEE Trans. Geosci. Remote Sens. 46 (10) (2008) 2924–2935.
[21] Yue Wanga, D.V. Rosowsky, Joint distribution model for prediction of hurricane wind speed and size, Struct. Saf. 35 (2012) 40–51.
[22] P.J. Vickery, F.J. Masters, M.D. Powell, D. Wadher, Hurricane hazard modeling: the past, present, and future, J. Wind Eng. Ind. Aerodyn. 97 (2009) 392–405.
[23] http://www.aoml.noaa.gov/hrd/data_sub/us_history.html
[24] G. Woo, The Mathematics of Natural Catastrophes, Imperial College Press, London, UK, 2007.
[25] http://www.nhc.noaa.gov
[26] S.D. Foss, S.H. Lin, R.A. Fernandes, Dynamic thermal line ratings – Part I. Dynamic ampacity rating algorithm, IEEE Trans. Power App. Syst. PAS-102 (June (6)) (1983) 1858–1864.
[27] H. Song, B. Lee, S.H. Kwon, V. Ajjarapu, Reactive reserve-based contingency constrained optimal power flow (RCCOPF) for enhancement of voltage stability margins, IEEE Trans. Power Syst. 18 (November (4)) (2003) 1538–1546.
[28] R.D. Zimmerman, C.E. Murillo-Sanchez, R.J. Thomas, MATPOWER: steady-state operations, planning, and analysis tools for power systems research and education, IEEE Trans. Power Syst. 26 (1) (2011) 12–19.
[29] Available at: http://www.ee.washington.edu/research/pstca/pf118/pg_tca118bus.htm (Online).